



Article

Two-Stage Anaerobic Codigestion of Crude Glycerol and Micro-Algal Biomass for Biohydrogen and Methane Production by Anaerobic Sludge Consortium

Sureewan Sittijunda ¹, Napapat Sitthikitpanya ², Pensri Plangklang ² and Alissara Reungsang ^{2,3,4,*}

¹ Faculty of Environment and Resource Studies, Mahidol University, Nakhon Pathom 73170, Thailand; sureewan.sit@mahidol.ac.th

² Biotechnology Program, Faculty of Technology, Khon Kaen University, Khon Kaen 40002, Thailand; napapat.sy@gmail.com (N.S.); penspl@kku.ac.th (P.P.)

³ Research Group for Development of Microbial Hydrogen Production Process from Biomass, Khon Kaen University, Khon Kaen 40002, Thailand

⁴ Academy of Science, Royal Society of Thailand, Bangkok 10300, Thailand

* Correspondence: alissara@kku.ac.th

Abstract: Optimization of factors affecting biohydrogen production from the codigestion of crude glycerol and microalgal biomass by anaerobic sludge consortium was conducted. The experiments were designed by a response surface methodology with central composite design. The factors affecting the production of hydrogen were the concentrations of crude glycerol, microalgal biomass, and inoculum. The maximum hydrogen production (655.1 mL-H₂/L) was achieved with 13.83 g/L crude glycerol, 23.1 g-VS/L microalgal biomass, and 10.3% (v/v) inoculum. The hydrogenic effluents obtained under low, high, and optimal conditions were further used as substrates for methane production. Methane production rates and methane yield of 868.7 mL-CH₄/L and 2.95 mL-CH₄/L-h were attained with the effluent produced under optimum conditions. The use of crude glycerol and microalgal biomass as cosubstrates had an antagonistic effect on biohydrogen production and a synergistic effect on methane fermentation. The two-stage process provided a more attractive solution, with a total energy of 1.27 kJ/g-VS_{added}, than the one-stage process.

Keywords: renewable energy; third generation biomass; anaerobic mixed cultures; dark fermentation; waste utilization



Citation: Sittijunda, S.; Sitthikitpanya, N.; Plangklang, P.; Reungsang, A. Two-Stage Anaerobic Codigestion of Crude Glycerol and Micro-Algal Biomass for Biohydrogen and Methane Production by Anaerobic Sludge Consortium. *Fermentation* **2021**, *7*, 175. <https://doi.org/10.3390/fermentation7030175>

Academic Editor:
Emmanuel Atta-Obeng

Received: 26 July 2021
Accepted: 28 August 2021
Published: 31 August 2021

Publisher's Note: MDPI stays neutral with regard to jurisdictional claims in published maps and institutional affiliations.



Copyright: © 2021 by the authors. Licensee MDPI, Basel, Switzerland. This article is an open access article distributed under the terms and conditions of the Creative Commons Attribution (CC BY) license (<https://creativecommons.org/licenses/by/4.0/>).

1. Introduction

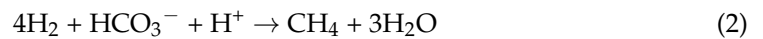
Increasing energy insecurity and environmental pollution caused by the overconsumption of fossil fuels is an emerging problem that is predicted to become very serious in the future [1]. Renewable energy sources such as wind, bioenergy (hydrogen and methane), and solar energy can be used to substitute fossil fuels, at least partially [1–4]. Of these, bioenergy has gained interest as a result of its cost-effectiveness. Biohydrogen and methane are promising energy carriers because of their high energy-generation capacity, environmental friendliness, and a wide variety of applicable feedstocks in their production processes [1–6]. The biohydrogen can be produced via dark fermentation and photo fermentation. However, owing to its lower energy consumption and a greater number of available feedstocks, dark fermentation has advantages over photo fermentation [7].

Moreover, this process generates various energy carriers, that is, hydrogen in the gaseous phase as well as aqueous ethanol and butanol. However, the main weakness of dark fermentation is its low hydrogen yield [8]. In general, 33% of a substrate can be converted into hydrogen [9], while the remaining substrate contributes to the production of microbial biomass and soluble metabolic products (SMPs); however, engineered strains of *Thermotoga maritima* can convert more than 33% of the substrate into hydrogen [10]. Hydrogen fermentation effluent or hydrogen effluents contain volatile fatty acids (VFAs) that

can be utilized as substrates to produce valuable products such as methane polyhydroxyalkanoate (PHAs) or to cultivate algal biomass [7,11]. Additionally, hydrogenic effluents have significant organic content and chemical oxygen demand (COD), which cannot be directly released into the environment without pretreatment or remediation. Therefore, anaerobic digestion (AD) of hydrogenic effluent to produce methane should be conducted to reduce the organic content and enhance the total energy recovery. Generally, substrates for methane production such as acetate, hydrogen, and carbon dioxide are obtained at the end of the hydrogen production process. These substrates are directly converted to methane via the pathways expressed in Equations (1) and (2) by methanogenic archaea. Other metabolites, such as propionate and butyrate, are cleaved into acetate and hydrogen via Equations (3) and (4), respectively. After that, the acetate and hydrogen through the reactions shown in Equations (1) and (2) are further converted to methane by methanogenic archaea via the acetoclastic and hydrogenotrophic cleavage pathways. One mole of acetic acid is converted to one mole of methane (Equation (1)) while 4 moles of hydrogen are converted to one mole of methane (Equation (2)).



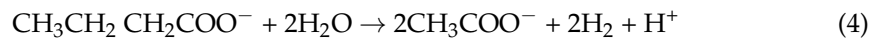
Acetoclastic methanogens



Hydrogenotrophic methanogens



Propionate oxidizing bacteria



Butyrate oxidizing bacteria

Crude glycerol is a waste stream from the processing of biodiesel. Typically, one kilogram of crude glycerol is produced with 10 kg of biodiesel [5,12]. Because of its high carbon content, crude glycerol can be used as a substrate to produce various kinds of biofuels, such as 1,3-propanediol (1,3-PD), hydrogen, and ethanol [5,12]. The current research used crude glycerol as a base for the production of hydrogen and methane. However, crude glycerol provides a low nitrogen source that cannot support microbial growth on its own [13]. Therefore, microalgal biomass with a high nitrogen content was used to codigest with crude glycerol to produce hydrogen and methane. Previous reports demonstrated successful production of methane through codigestion of microalgal biomass (*Chlorella* sp, *Arthrospira platensis*, and *Platymonas subcordiformi*) were with other substrate in the AD process [14–17]. Among these, *Chlorella* sp. demonstrated a high improvement potential to codigest with other substrate such as sewage sludge [16,17], crude glycerol [13], septic sludge [17], and macroalgal biomass [15]. However, there is still a lack of knowledge on the codigestion of microalgal biomass and crude glycerol in two-stage biohydrogen and methane processing. Thus, this study aims to explore the possibility of using algal biomass as a cosubstrate with crude glycerol for two-stage biohydrogen and methane production.

Optimization of environmental factors, including substrate and inoculum concentrations, is required to optimize the production of biohydrogen from the codigestion process. The identification of an optimal concentration of substrate and inoculum and the correlation between variables were conducted using response surface methodology with central composite design (RSM with CCD). In addition, methane production from hydrogenic effluent using mixed anaerobic cultures was also investigated. Finally, bacterial communities were studied using polymerase chain reaction with denaturing gradient gel electrophoresis (PCR-DGGE).

2. Materials and Methods

2.1. Substrates

Glycerol waste was received from CPF Public Co., Ltd., Chokchai District, Nakhon Ratchasima Province, Thailand, from a biodiesel production process. This firm supplies processed poultry meat and produces 202.60 tons of waste oil per month on average. Approximately 22,000 L of biodiesel with 2200 L of crude glycerol is produced monthly by this transesterification process. Crude glycerol compositions have been reported at Sittijunda and Reungsang [18].

Dry *Chlorella* sp. powder was received from the Research Group of Development of Microbial Hydrogen Production Process from Biomass, Khon Kaen University, Khon Kaen, Thailand. The chemical compositions of *Chlorella* sp. including carbohydrate, protein, lipid, and ash were determined using AOAC standard methods [19]. In addition, amino acid content was analyzed using high-performance liquid chromatography (HPLC). The compositions of *Chlorella* sp. were previously reported by Phanduang, et al. [20]. Dry powder of *Chlorella* sp. was placed in an airtight plastic bag at $-20\text{ }^{\circ}\text{C}$ until use.

2.2. Inoculum Preparation

Anaerobic granules were obtained from a system for treating wastewater in internal circulation (IC). For this biohydrogen development experiment, the IC granules were washed twice using tap water and then soaked in distilled water for 3 days to eliminate impurities and residual nutrients. They were then heated to $105\text{ }^{\circ}\text{C}$ for 2 h to deactivate methanogens. Subsequently, 50 g of heated IC granules was added into 500 mL glass bottles containing 350 mL of 25 g/L pure glycerol as the carbon source, combined with an Endo-nutrient solution [21]. The initial pH was adjusted to 6.0 using 5 M HCl. To establish anaerobic conditions, it was capped with rubber stoppers and flushed with nitrogen gas for 10 min before placing on the orbital shaker at 150 rpm and incubated at room temperature ($35 \pm 4\text{ }^{\circ}\text{C}$). A total of 175 mL (50%) of culture broth was replaced by 25 g/L pure glycerol and Endo-nutrient solution every 3 days. The replacement process was conducted until a constant initial cell concentration (g-volatile suspended solids (VSS)/L) was observed (subcultured 7 times). The culture was further used as a seed inoculum for biohydrogen production.

For the methane production trial, the IC granules were washed with tap water twice and then immersed in distilled water for 3 days. They were then air-dried and kept at $4\text{ }^{\circ}\text{C}$ until usage. Initial concentrations of cells were calculated as g-VSS/L and recorded.

2.3. Central Composite Design (CCD)

CCD was used to optimize the level of three variables, i.e., crude glycerol concentration (g/L) (X_1), inoculum concentration (%v/v) (X_2), and algal biomass concentration (g-VS/L) (X_3). These three variables were standardized at the confidence level of 95 percent. According to our previous study, the selected ranges for crude glycerol and inoculum should be 0–40 g/L and 10–30% (v/v) [22,23]. For the algal biomass, the selected range was 5–20 g-VS/L [24]. The response variable was an average value of hydrogen production (mL- H_2 /L). For statistical analysis, test factors of X_i are coded as x_i as shown in the following equation:

$$x_i = (X_i - X_0) / \Delta X_i \quad (5)$$

where X_i is the actual value of the independent variable; x_i is the coded value of the variable X_i ; X_0 is the value of X_i at the center point, and ΔX_i is the step change value. A quadratic model (Equation (6)) is used to optimize the factors

$$Y = \beta_0 + \sum \beta_i X_i + \sum \beta_{ii} X_i^2 + \sum \beta_{ij} X_i X_j \quad (6)$$

where Y is the predicted response; β_0 is a constant; β_i is the linear coefficient; β_{ii} is the squared coefficient; β_{ij} is the interaction coefficient; and X_i is the variable. The response variable was fitted using a predictive polynomial quadratic equation (Equation (6)) to

correlate the response to the independent variables [25]. The statistical software Design-Expert (Demo version 7.0, Stat-Ease, Inc., Minneapolis, MN, USA) is used for regression and graphical analysis of the experimental data. The right consistency of the quadratic model is represented by the determination coefficient, R^2 , and the F-test was used to verify its significance. The conditions of each trial are shown in Table 1.

Table 1. Central composite design matrix defining the concentration of crude glycerol (X_1), the concentration of inoculum (X_2), and the concentration of algal biomass (X_3) and their effect on the production of hydrogen.

Run	Glycerol Concentration (X_1)		Inoculum Concentration (X_2)		Algal Biomass Concentration (X_3)		Hydrogen Production	
	(g/L)		(% v/v)		(g-VS/L)		(mL-H ₂ /L)	
	Code	Actual	Code	Actual	Code	Actual	Observed	Predicted
1	1	40	1	25	−1	4.62	5.76 ± 0.73	5.5
2	−1	10	1	25	1	23.1	583.2 ± 3.76	551.2
3	0	25	−1	6.17	−1	4.62	53.6 ± 2.77	56.5
4	0	25	1.628	31.39	0	13.86	210 ± 4.25	205.3
5	0	25	0	15.63	0	13.86	459.4 ± 1.05	458.2
6	−1.682	0	0	15.63	0	13.86	11.4 ± 0.04	11.5
7	0	25	0	15.63	0	13.86	459.4 ± 1.05	458.2
8	0	25	0	15.63	0	13.86	459.4 ± 1.05	458.2
9	1	10	1	6.17	−1	23.1	702.7 ± 1.28	717.9
10	1.628	50.23	0	15.63	0	13.86	295.5 ± 0.46	282.2
11	−1	10	1	25	−1	4.62	9.9 ± 0.16	10
12	1	40	1	25	1	23.1	311.1 ± 0.81	312.9
13	0	25	0	15.63	0	13.86	459.4 ± 1.05	458.2
14	0	25	0	15.63	0	13.86	459.4 ± 1.05	458.2
15	−1	10	−1	6.17	−1	4.62	311.1 ± 1.03	318.8
16	0	25	0	15.63	1.628	29.4	530.7 ± 2.20	575.2
17	1	40	−1	6.17	1	23.1	73.7 ± 3.57	75.9
18	0	25	0	15.63	0	13.86	459.4 ± 1.05	458.2
19	0	25	−1.628	0	0	13.86	58.4 ± 0.34	55.3
20	0	25	0	15.63	−1.628	0	15.9 ± 0.04	15.6

2.4. Confirmation Experiment

In the confirmation experiment, the model, the predicted conditions for optimizing hydrogen production (optimum conditions), low and high conditions, were further used for the model validation. The control experiment was crude glycerol with inoculum and algal biomass with inoculum at the optimum level. The initial pH in each experiment was set to 6.0. All treatments were done in triplicate.

2.5. Biohydrogen Production Experiments

The production of biohydrogen was carried out in serum bottles of 120 mL with 70 mL working volumes. The production medium contained crude glycerol, an inoculum solution, algal biomass, and Endo-nutrient. Endo-nutrient was used to supply nutrients at a rate of 6 mL/L of the substrate. Its compositions were previously reported by Lin and Lay [21]. Concentrations of crude glycerol, inoculum, and algal biomass were set using a CCD design. Table 1 shows the experimental conditions of each trial. In each experiment, the initial pH was adjusted to 6.0. The serum bottles were lined with rubber stoppers and caps made of aluminum. Instead, to establish anaerobic conditions, the headspaces of the serum bottles were flushed with nitrogen gas. Then, the serum bottles were incubated on the orbital shaker at 150 rpm, and at room temperature (35 ± 4 °C). All treatments were carried out in triplicate. The amount of biogas was measured during the incubation using a wetted glass syringe method [26]. Measures on the production of hydrogen continued until the production of biogas ceased.

2.6. Methane Production from the Hydrogenic Effluent of a Biohydrogen Production Process

The remaining hydrogenic effluents from the biohydrogen production process under low, high, and optimum conditions, as described in the experimental design, were used to produce methane for the recovery of additional energy from the codigestion of crude glycerol and algal biomass. IC granules were applied as inoculum at a concentration of 25 g-VSS/L. Methane production was carried out in serum bottles of 120 mL with a working volume of 70 mL. The fermentation included hydrogenic effluents and inoculum. The pH was adjusted to 7.5 with the addition of either 1 N NaOH or 1 N HCl as required. The establishment of anaerobic conditions, the volume of gas emitted, and the determination of the composition of the gas were carried out as outlined in the section on biohydrogen production.

2.7. Analytical Methods

Biogas parameters, including its hydrogen, methane, nitrogen, and carbon dioxide contents, were determined using a gas chromatograph (GC, Shimadzu 2014, Japan) fitted with a thermal conductivity detector (TCD) and a column lined with shin carbon (50/80 mesh). The operation conditions of GC-TCD conditions were set according to Sittijunda and Reungsang [18]. In brief, a 2 m stainless column packed with shin carbon (50/80 mesh) was used. The injector, detector and column oven temperatures were 100, 120, and 150 °C, respectively. Helium was used as a carrier gas at a flow rate of 25 mL/min. The pH was measured with a digital pH meter (Sartorius, Germany). The hydrogen and methane production rates were calculated using the modified Gompertz equation [27]. The fermentation broths from the experiments that produced the highest and lowest hydrogen and methane were collected to extract DNA for the study of the microbial community using PCR-DGGE. The PCR-DGGE conditions were established as previously described by Sreela-or, et al. [28]. The analysis of VFA was determined by HPLC, as mentioned above, by Sittijunda and Reungsang [12]. Briefly, the liquid samples were precipitated with 34% (v/v) H₃PO₄, centrifuged at 12,000 rpm for 5 min, acidified with 0.2 N oxalic acid, and filtered over a 0.45 mm nylon membrane filter. The resultant filtrate was analyzed by HPLC with the refractive index (RI) detector using a Vertiseq™ OA 8 µm column. The column was operated at 40 °C, with 4 mM H₂SO₄ being used as the mobile phase at a flow rate of 0.5 mL/min. Inoculum to substrate ratio (ISR) was calculated based on terms of gram volatile solid (VS) of inoculum divided by gram volatile solid of substrate. Carbon to nitrogen ratio (C/N ratio) was calculated from the carbon and nitrogen contents presented in crude glycerol and algal biomass.

The potential synergistic and antagonistic effects (α value) occurred during the hydrogen and methane production processes were reported by Sittijunda and Reungsang [18]. Energy balance (E_{bal} , kJ/g-VS) was calculated by minus energy output (E_{out} , kJ/g-VS) with energy input (E_{in} , kJ/g-VS). The output energy from hydrogen and methane (kJ/g-VS) was calculated by multiplying hydrogen (mL-H₂/g-VS_{added}) and methane yields (ml-CH₄/g-VS_{added}) with relative hydrogen densities (0.089 mg-H₂/mL-H₂) and methane densities (0.72 mg-CH₄/mL-CH₄) and then multiplying with hydrogen heating values (121 kJ/g-H₂) and methane heating value (50 kJ/g-CH₄) [18]. Input energy was the energy used for shaking process. The input energy was calculated using Equation (7) [20].

$$E_{in} = \frac{P_d \times t \times 3.6}{C_s} \quad (7)$$

where P_d is the device power energy (150 watts for shaker), 3.6 is the conversion factor for converting from 1 watt to kJ/h, t is the time (h), and C_s is the substrate concentration.

3. Results and Discussion

3.1. Biohydrogen Production from a Codigestion of Crude Glycerol with Algal Biomass Using RSM with CCD

The results showed that the expected hydrogen production values were in near agreement with the experimental data (Table 1). Equation (8) represents the regression by fitting experimental data on the production of hydrogen.

$$\begin{aligned} \text{Hydrogen production} = & 136.19 + 107.78X_1 - 766.74X_2 + 275.62X_3 \\ & + 192.49X_1X_2 - 79.93X_1X_3 + 135X_2X_3 - 91.32X_1^2 - 455.31X_2^2 - 58.28X_3^2 \end{aligned} \quad (8)$$

Hydrogen production ranged from 5.8 mL to 702.7 mL-H₂/L. The maximum hydrogen production, 702.7 mL-H₂/L, was obtained at crude glycerol, inoculum, and algal biomass concentrations of 10 g/L, 6.17% (v/v), and 23.10 g-VS/L, respectively (Run 9). The lowest hydrogen production was found at crude glycerol, inoculum, and algal biomass concentrations of 40 g/L, 25% (v/v), and 4.62 g-VS/L, respectively (Run 1). ANOVA results of the obtained model revealed a low *p*-value of 0.0178, suggesting that the model adequately fits the data (Table 2). A high coefficient of determination ($R^2 = 0.92$) indicates that the model covers 92% of the response variability. The *p* values in these models determined the importance of the variables. Linear terms of inoculum and algal biomass concentrations significantly affected the production of hydrogen (*p* < 0.05, Table 2). Quadratic terms glycerol (X_1^2) and inoculum (X_2^2) were highly significant (*p* < 0.05). Maximum hydrogen production of 612 mL-H₂/L was achieved at a glycerol concentration of 13.83 g/L, an algal biomass concentration of 23.1 g-VS/L, and an inoculum concentration of 10.3% (v/v) (optimum condition).

Table 2. ANOVA of the fitting model for hydrogen production.

Source	Sum of Squares	df	Mean Square	F Value	<i>p</i> -Value Prob > F
Model	760,000.00	9	84,383.99	4.19	0.0178
X ₁	22,357.92	1	22,357.92	1.11	0.3171
X ₂	126,000.00	1	126,000.00	6.23	0.0317
X ₃	145,000.00	1	145,000.00	7.18	0.0231
X ₁ X ₂	55,798.53	1	55,798.53	2.77	0.1272
X ₁ X ₃	51,115.31	1	51,115.31	2.54	0.1424
X ₂ X ₃	27,439.96	1	27,439.96	1.36	0.2704
X ₁ ²	118,000.00	1	118,000.00	5.85	0.0361
X ₂ ²	143,000.00	1	143,000.00	7.08	0.0238
X ₃ ²	41,327.48	1	41,327.48	2.05	0.1827
Residual	202,000.00	10	20,163.01		
Lack of Fit	202,000.00	5	40,326.03		

Figure 1A–C represents three-dimensional surface plots with fixing one variable at their center values while varying the other two parameters within the range of their experimental values. The correlations between concentrations of crude glycerol and inoculum, as well as crude glycerol and algal biomass in hydrogen production, are seen in Figure 1A,B, respectively. At 13.86 g-VS/L of algal biomass concentration, hydrogen production increased due to the increased crude glycerol concentrations from 10 to 25 g/L (Figure 1B). Further increase in crude glycerol concentration to levels higher than 25 g/L caused a drop in hydrogen production. A drop in hydrogen production could be due to the impurities contained in crude glycerol such as methanol, soap, salt (NaCl), and fatty acid [29,30]. Bacterial growth and metabolism are affected by methanol at concentrations equal to or greater than 10 g/L [31]. In addition, crude glycerol used in this study contains high concentration NaCl (8.93 g/L) and methanol (230 g/L), and thus, a high concentration of crude glycerol could contribute to a high concentration of NaCl which are toxic to microbes. These results show that the optimal concentration of crude glycerol should be between

10 and 25 g/L. Therefore, the use of suitable crude glycerol concentrations is needed to maximize the activity of fermentative bacteria and hydrogen production.

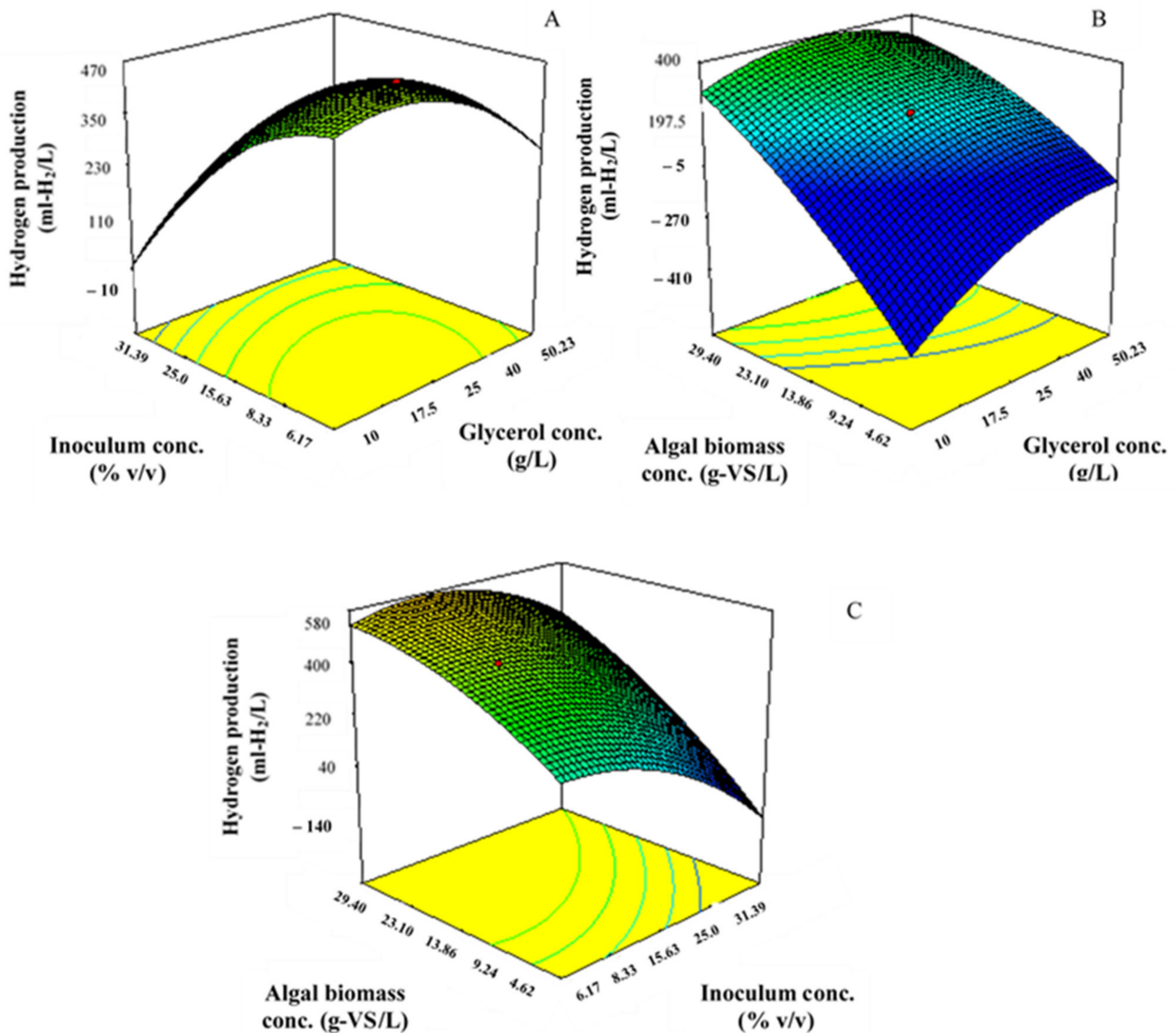


Figure 1. Surface plots showing the effects of crude glycerol and inoculum on hydrogen production and their interactive effects at 13.86 g-VS/L of algal biomass (A); the effect of algal biomass, crude glycerol, and interactive effect at 15.63% (v/v) of inoculum concentration (B); the effect of algal biomass, inoculum, and interactive effect at crude glycerol of 25 g/L (C).

Figure 1A,C shows the variation of hydrogen production values affected by inoculum concentrations ranging from 0 to 25% (v/v) equal to 0 to 14.36 g-VSS/L. The results show that the variation in inoculum concentrations causes hydrogen production fluctuations. Hydrogen production decreased with an increased inoculum concentration higher than 6.17% (v/v) (Figure 1A,C). The concentration of inoculum is a crucial parameter that affects the degradation rate of organic matter in dark fermentation [32,33]. To maximize the production of hydrogen, the inoculum level should thus be kept in the desired range. Moreover, a variation in the inoculum also impacted the inoculum to substrate ratio. At ISR of 0.37, a hydrogen production of 9.9 mL-H₂/L was observed (Run 11). A decrease in the ISR from 0.37 to 0.03 (Run 9) increased hydrogen production from 9.9 to 702.7 mL-H₂/L. These results indicate that a reduction in hydrogen production might be caused by an imbalance between the inoculum and substrate concentrations.

Figure 1B,C shows the relationships between the concentrations of algal biomass and crude glycerol and the concentrations of algal biomass and inoculum, respectively. At a fix inoculum concentration of 15.63% (*v/v*), an increase in algal biomass above 4.62 g-VS/L resulted in an increase in hydrogen production (Figure 1B). In addition, a fix crude glycerol concentration of 25 g/L, the algal biomass concentration was increased to greater than 29.40 g-VS/L resulted in an increase in hydrogen production (Figure 1C). Resultantly, the optimal level of algal biomass concentration that provided the best hydrogen production was not observed. Therefore, in order to determine the optimal or inhibition level of algal biomass concentration, the experimental setup should be carried out at a concentration of algal biomass greater than 29.40 g-VS/L. Algal biomass serves as a nitrogen source that can be used as components of nucleic acids, enzymes, and proteins in microbial cells [18]. At the setting ranges, an inhibitory effect of algal biomass as a nitrogen source was not observed. Moreover, *Chlorella* sp. (Chlorophytes) used in this study contains carbohydrates (29.17% *w/w*), lipids (8.66% *w/w*), and amino acids such as glutamic acid, aspartic acid, and lysine [34] that can encourage the microbial growth and activity.

3.2. Confirmation Experiments

Verification tests were conducted to validate the statistical model under optimum, low, and high conditions (Table 3). Under the optimum conditions, the hydrogen production was slightly increased from 0 to 40 h, and then sharply increased after 40 h (Figure 2) implying that the microorganisms took time to adapt themselves to metabolite crude glycerol and algal biomass for hydrogen production. This finding was supported by the long lag time (λ) of 39 h under the optimum conditions. Hydrogen production of 655.1 mL-H₂/L was achieved under optimum conditions (Table 3). Studies have shown that this value was 7.03% away from the estimated value (612 mL-H₂/L). Under the optimal conditions, a maximal hydrogen production rate (HPR) of 4.1 mL-H₂/L-h was obtained, which was 1.05 and 2.56 times higher than that under low and high conditions, respectively (Table 3). The results suggested that appropriate levels of crude glycerol, inoculum, and algal biomass could improve the microbial community, which enhanced hydrogen production and HPR. The primary VFA was propionic acid with smaller concentrations of butyric, and acetic acids (Figure 3). At the end of fermentation process, the pH was reduced to 5.5–5.75 (data not shown) due to an accumulation of VFAs. The presence of NaHCO₃ and NH₄HCO₃ in the Endo-nutrient prevented the dramatically decrease of pH during the hydrogen production process [35]. Our results showed that production pathways during hydrogen production were butyrate- and acetate-type fermentations [36,37]. This result coincided with the study Choi and Ahn [38] who found that at the pH 5 to 9, butyrate was the most dominant product followed by acetate. The production of propionic acid decreased hydrogen production since its formation consumes hydrogen [36,37].

Table 3. Hydrogen production, HPR, and total volatile fatty acid (TVFAs) production at low, high, and optimal conditions from codigestion of crude glycerol and algal biomass.

Experiment	Glycerol Concentration (g/L)	Inoculum Concentration (% <i>v/v</i>)	Algal Biomass Concentration (g-VS/L)	Hydrogen Production (mL-H ₂ /L)	HPR (mL-H ₂ /L h)	TVFAs (g/L)
Low	10.00	6.17	4.62	252.56 ± 2.27	3.98	8.44 ± 3.67
High	40.00	25	23.1	140.67 ± 3.41	1.60	11.94 ± 2.36
Optimum	13.83	10.31	23.1	655.12 ± 1.64	4.07	13.28 ± 3.06

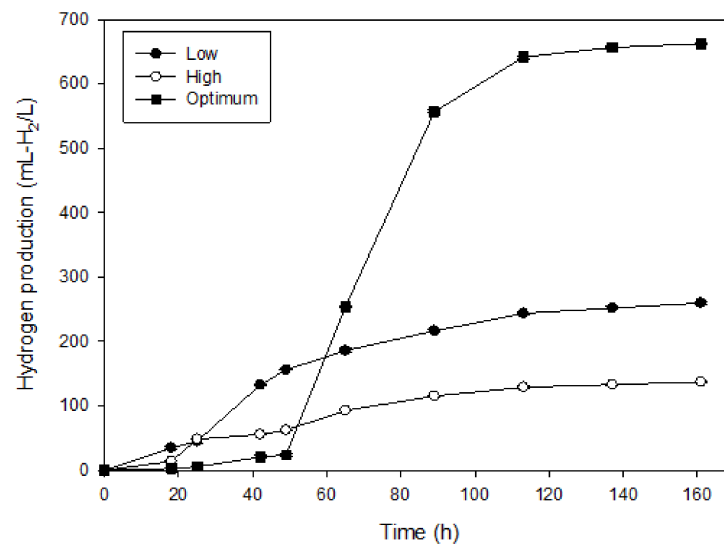


Figure 2. Time course profile of hydrogen production from a codigestion of crude glycerol with algal biomass at the initial pH of 6 at low (10 g/L of glycerol, 6.17% of inoculum, and 4.62 g-VS/L of algal biomass), high (40 g/L of glycerol, 25% of inoculum, and 23.1 g-VS/L of algal biomass), and optimal (13.83 g/L of glycerol, 10.31% of inoculum, and 23.1 g-VS/L of algal biomass) conditions.

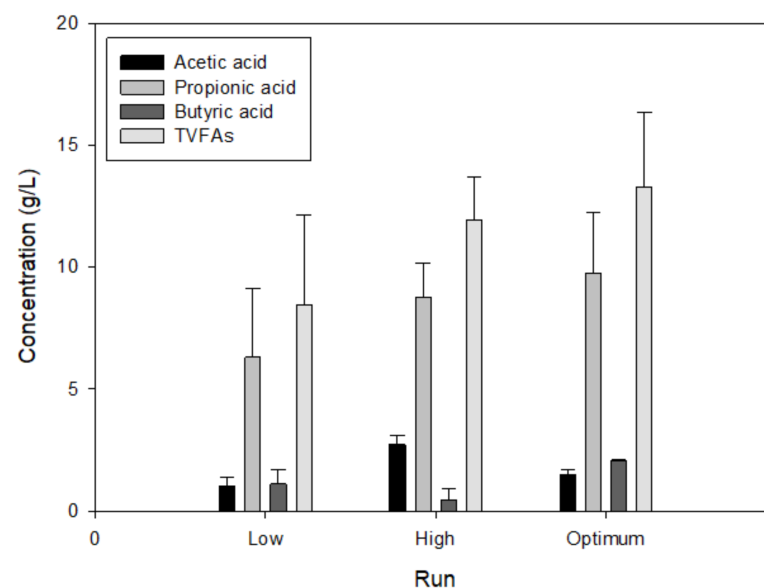


Figure 3. VFA production from a codigestion of crude glycerol with algal biomass at the initial pH of 6 under low (10 g/L of glycerol, 6.17% of inoculum, and 4.62 g-VS/L of algal biomass), high (40 g/L of glycerol, 25% of inoculum, and 23.1 g-VS/L of algal biomass), and optimal (13.83 g/L of glycerol, 10.31% of inoculum, and 23.1 g-VS/L of algal biomass) conditions. TVFA: total volatile fatty acid.

A comparison of the HY obtained in this study with those reported in the literature is shown in Table 4. The HY obtained in this study was comparable with Fountoulakis and Manios [39] and Kanchanasuta and Sillaparassamee [40] but lower than that in other studies [41,42] (Table 4). This outcome might have been due to the difference in C/N ratios, inoculum types, and fermentation conditions of these studies. In the current study, the C/N ratio varied over the range from 0.9 to 5.8. This C/N ratio was quite low compared to previous reports [40,42]. Nitrogen can accumulate in the form of ammonium (NH_4^+) ions. High concentrations of ammonium ions inhibit biohydrogen production, probably by altering the intracellular pH of hydrogen-producing bacteria and increasing the en-

ergy required for cell maintenance or by inhibiting specific enzymes related to hydrogen production, such as hydrogenase [40,42].

Table 4. Comparison of hydrogen yields from this study with those reported in the literature.

Raw Materials	Organisms	Hydrogen Yield (mL/g-VS _{added})	Reference
Synthetic organic fraction of municipal solid waste + 1% glycerol	Anaerobic sludge	26	Fountoulakis and Manios [39]
Mixture of olive mill wastewater and slaughterhouse wastewater + 1% glycerol	Anaerobic digester sludge	15	Fountoulakis and Manios [39]
Palm oil decanter cake + 1.5% glycerol	Anaerobic sludge	23	Kanchanasuta and Sillaparassamee [40]
Food waste + 1% glycerol	Anaerobic digested sludge	140	Silva, Oliveira, Mahler, and Bassin [41]
Food waste + 3% glycerol	Anaerobic digested sludge	176	Silva, Oliveira, Mahler, and Bassin [41]
Industrial municipal solid waste + 1% glycerol	Thermophilic anaerobic digester effluent	51	Zahedi, Solera, García-Morales, and Sales [42]
Crude glycerol + algal biomass	Anaerobic mixed cultures	21.68	This study

3.3. Methane Production from the Hydrogenic Effluent of a Biohydrogen Production Process

Methane production (MP) from the hydrogenic effluent under low, high, and optimal conditions is depicted in Figure 4. Under all of these conditions, the methane production increased with incubation time. Under optimal conditions, methane production dramatically increased after 90 h of fermentation (Figure 4). This is because the microbials took a long time to adapt themselves to the high concentration of TVFAs which indicated by a long lag time (λ) of 94 h. Additionally, an accumulation of a high concentration of propionic acid (9.74 g/L) resulted in a low methanogenic activity. It is worth noting that this concentration does not exceed the inhibitory level of 30 g/L [43]. An average methane content of 20–50% (*v/v*) was founded at all experimental conditions. Another gas produced during the two-stage anaerobic digestion was carbon dioxide with an average content of 50–80% *v/v*. The highest methane production was found under optimal conditions. MP and methane production rate (MPR) values of 387.4 mL-CH₄/L and 1.34 mL-CH₄/L-h were obtained when using the hydrogenic effluent from the low condition. Increases in the MP and MPR to 428 mL-CH₄/L and 1.40 mL-CH₄/L-h, respectively, were found when using the effluent of the high condition for the hydrogen production process as a substrate (Table 5). The maximal MP and MPR, 868.7 mL-CH₄/L and 2.95 mL-CH₄/L-h, respectively, were obtained when using the effluent of hydrogen fermentation under optimal conditions. Under low, high, and optimal conditions, propionic acid was the primary VFA (Figure 3). It was cleaved into acetic acid by propionate-oxidizing bacteria (Equation (2)). After that, it was further used to produce methane by acetoclastic methanogenic archaea (Equation (3)). The results suggested that variations in MP and MPR might be caused by changes in the TVFA concentrations and types of VFAs in each fermentation broth.

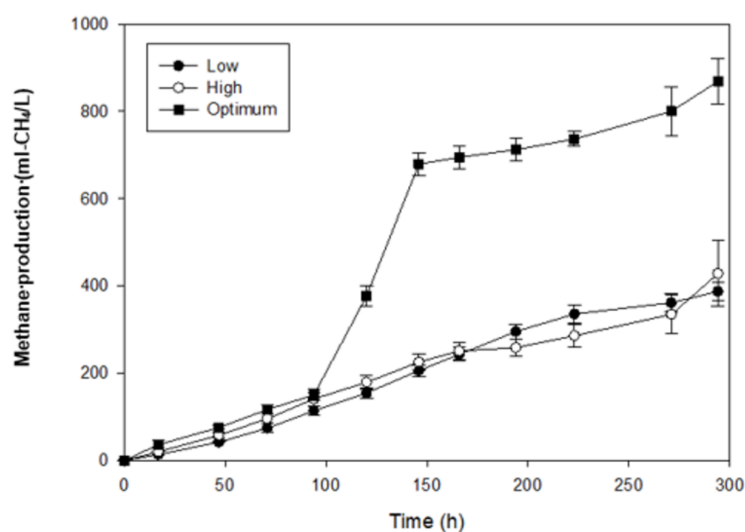


Figure 4. Time course profile of methane production from the hydrogenic effluent of crude glycerol codigested with algal biomass at the initial pH of 7.5 at low (10 g/L of glycerol, 6.17% of inoculum, and 4.62 g-VS/L of algal biomass), high (40 g/L of glycerol, 25% of inoculum, and 23.1 g-VS/L of algal biomass), and optimal (13.83 g/L of glycerol, 10.31% of inoculum, and 23.1 g-VS/L of algal biomass) conditions.

Table 5. MP and MPR using the hydrogenic effluent as substrates from low, high, and optimal conditions.

Hydrogenic Effluent	MP (mL-CH ₄ /L)	MPR (mL-CH ₄ /L-h)
Low	387.4 ± 20.04	1.34
High	428.0 ± 13.12	1.40
Optimum	868.7 ± 19.98	2.95

The maximum MP and MPR (868.7 mL-CH₄/L and 2.95 mL-CH₄/L-h) obtained in this study was higher than that in one-stage anaerobic codigestion of microalgal biomass with crude glycerol (58.88 mL-CH₄/L and 0.37 mL-CH₄/L-h) [18]. In contrast, it was lower than that reported from the using of hydrogenic effluent obtained from pretreated Napier grass (5960 mL-CH₄/L and 370 mL-CH₄/L-d), pretreated Napier silage (5643 mL-CH₄/L and 370 mL-CH₄/L-d) [44], and palm oil mill effluent (3.2 L-CH₄/L-d) and as the substrate [45]. This outcome might have been due to a difference in effluent compositions, inoculum types, and fermentation conditions of these studies.

In addition, a drop of pH at the end of fermentation process (pH of 5; data not shown) may inhibit the methanogenic bacteria. A drop of pH in the AD process could be caused by an absent of buffer substance in the hydrogenic effluent. Therefore, in order to improve the production efficiency, an additional of buffer substance as well as trace element could be carried out.

3.4. Microbial Communities

The PCR-DGGE analysis of the bacterial and archaeal populations is presented in Figure 5A,B. These tests were performed at the end of hydrogen and methane production from the codigestion of crude glycerol with algal biomass. Lanes G and H depict the bacterial communities found under low and optimum conditions of hydrogen production from the codigestion of crude glycerol with algal biomass. Lanes I and J depict the archaeal community observed under low and optimum conditions for methane production from the codigestion of crude glycerol with algal biomass, respectively.

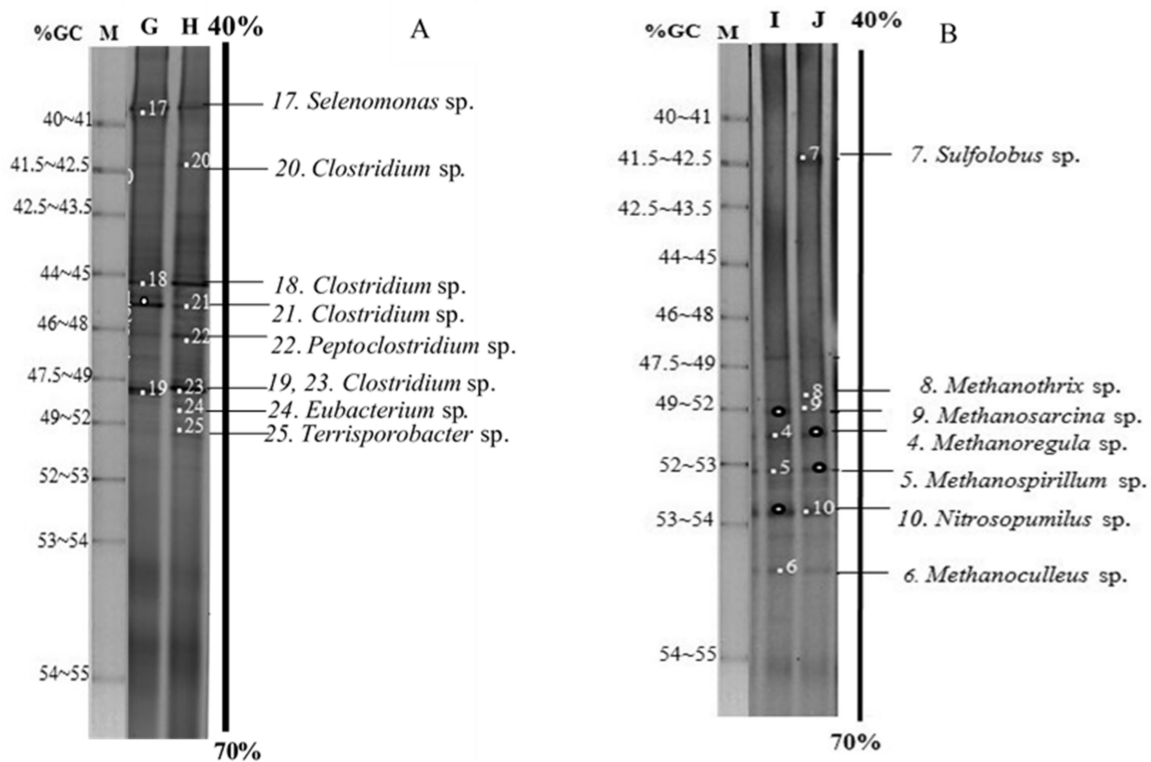


Figure 5. DGGE profiles of 16S rDNA fragments for the bacterial (A) and archaeal (B) species after hydrogen and methane production from the codigestion of crude glycerol with algal biomass at the optimum lanes: G, I and low conditions lanes: H, J.

In the hydrogen production stage, the bacterial population found under low and optimum conditions was *Clostridium* sp. (Bands 18, 19, 20, 21, and 23) *Eubacterium* sp. (Band 24), *Peptoclostridium* sp. (Band 22), *Selenomonas* sp. (Band 17), and *Terrisporobacter* sp. (Band 25). All the bacterial populations except *Selenomonas* sp. (Band 17) and *Terrisporobacter* sp. (Band 25) were hydrogen-producing bacteria. *Selenomonas* sp. (Band 17) and *Terrisporobacter* sp. (Band 25) were reported as propionic- and acetic-producing bacteria [46]. Initially, all bacterial populations converted crude glycerol and algal biomass into small molecules such as sugar amino acids and fatty acids. Afterward, the leading hydrogen-producing bacteria, including *Clostridium* sp. (Bands 18, 19, 20, 21, and 23), *Eubacterium* sp. (Band 24), and *Peptoclostridium* sp. (Band 22) converted small molecules into hydrogen and carbon dioxide in the gas phase and VFAs in the liquid phase. *Selenomonas* sp. (Band 17) and *Terrisporobacter* sp. (Band 25) were the primary acid-producing bacteria in the fermentation broth. Both species converted small molecules into high concentrations of propionic and acetic acids in the fermentation broth.

The dominant bacteria founded in the anaerobic sludge obtained from the brewery wastewater treatment process were *Clostridia*, *Epsilonproteobacteria*, *Anaerolineae*, *Streptococcus*, and *Betaproteobacteria* [47]. Among these, *Clostridia* were reported as hydrogen producing bacteria. In contrast, *Methanosaeta* and *Methanobacterium* were the dominant archaea genera founded in granule samples [48]. These genera were reported as methane producers using acetate and hydrogen as the substrate.

For the methane production stage, the archaeal populations were *Methanoregular* sp. (Band 4), *Methanospirillum* sp. (Band 5), *Methanoculleus* sp. (Band 6), *Sulfolobus* sp. (Band 7), *Methanothrix* sp. (Band 8), *Methanosarcina* sp. (Band 9), and *Nitrosopumilus* sp. (Band 10). All the archaea populations, except *Sulfolobus* sp. (Band 7) and *Nitrosopumilus* sp. (Band 10), were methanogenic bacteria that converted acetate, hydrogen, and carbon dioxide into methane. In Figure 5, *Methanothrix* sp. (Band 8) and *Methanosarcina* sp. (Band 9) were detected as the main methane producers in the codigestion of crude glycerol with algal

biomass via an acetoclastic pathway, Equation (1). *Methanoregular* sp. (Band 4), *Methanospirillum* sp. (Band 5), and *Methanoculleus* sp. (Band 6) are the methanogens utilizing hydrogen and carbon dioxide as substrates for methane production via the hydrogenotrophic pathway, Equation (2). *Nitrosopumilus* sp. (Band 10) is an ammonia-oxidizing bacterium capable of converting inorganic nitrogen into its oxidized forms [49]. *Sulfolobus* sp. (Band 7) is an acidophile that thrives in aerobic condition at a pH of 2–3 [50] under aerobic conditions. *Sulfolobus* sp. can use cellulose, hexose, pentose sugars, and amino acid as carbon sources [50]. According to our results, methanogenesis occurred through acetoclastic and hydrogenotrophic cleavage pathways.

The hydrogen- and methane-producing bacteria present under low and optimum conditions were not diverse in terms of species; however, they were diverse in terms of band intensities (Figure 5). The results suggest that controlling environmental factors such as substrates, temperature, and pH are sufficient to prevent microbial diversity changes. The diverse in band intensities are caused by the environmental factors including the concentrations of crude glycerol, inoculum size, amount of algal biomass and others.

3.5. Synergistic or Antagonistic Effects during Hydrogen and Methane Production

Some combinations of substrates to produce hydrogen and methane show synergistic and antagonistic effects. Both effects define the relationship between the microorganisms, either in complementing or hindering one another during the codigestion process [51]. The possible synergistic or antagonistic effects in hydrogen and methane production are calculated as mentioned in Sittijunda and Reungsang [18]. When crude glycerol was utilized with algal biomass, the hydrogen yield was lower than when using a single substrate, and the α value was less than 1 ($\alpha = 0.63$) (Table 6). Hence, antagonism is seen in this fermentation. This result might be due to an imbalance in the C/N ratio. It could also be due to a deficiency, an excess, or an imbalance in the ratios of trace elements or ammonia toxicity [51]. In contrast, the α value obtained from methane production was greater than codigestion of crude glycerol with algal biomass, which is more productive in terms of methane yield compared to fermentation of a single substrate. This result indicates a synergistic effect during the methane production process.

Table 6. The interaction effects during two-stage hydrogen and methane production under optimal conditions.

Experiment	Glycerol Concentration		Inoculum Concentration	Algal Biomass Concentration	Yield	α^*
	(g/L)	(g-VS/L)	(%v/v)	(g-VS/L)	(mL/g-VS _{added})	
Hydrogen						
Optimal	13.83	7.12	10.3	23.1	21.68	0.63
	13.83	7.12	10.3	0	23.33	
	0	0	10.3	23.1	11.24	
Methane						
Optimal	13.83	7.12	25	23.1	28.75	1.05
	13.83	7.12	25	0	17.21	
	0	0	25	23.1	10.09	

* The calculation of α value was shown in Section 2.5.

3.6. Energy Production in Two-Stage Hydrogen and Methane Production from a Single Substrate and Codigestion of Crude Glycerol and Algal Biomass and Energy Balance

The energy production in two-stage hydrogen and methane production from the codigestion of crude glycerol and algal biomass and single digestion of crude glycerol or algal biomass only under the optimum conditions is depicted in Figure 6. Total energy production of 1.27, 0.87, and 0.49 kJ/g-VS_{added} was obtained from codigestion and single digestion of crude glycerol and algal biomass as the substrate, respectively. The total energy production from a codigestion process (1.27 kJ/g-VS_{added}) was higher than that

using a single digestion of crude glycerol ($0.87 \text{ kJ/g-VS}_{\text{added}}$) or algal biomass ($0.49 \text{ kJ/g-VS}_{\text{added}}$) only. This means that the combination of crude glycerol and algal biomass provides a better situation that enhances the microbial activity in which a maximum total energy production is obtained. Single digestion of crude glycerol gave better energy production than using algal biomass alone (Figure 6). The results showed that the activity of hydrogen-producing bacteria when using algal biomass alone was lower than when using crude glycerol alone as the substrate. Furthermore, the energy production obtained in this study ($1.27 \text{ kJ/g-VS}_{\text{added}}$) was higher than that from one-stage methane production from a codigestion of crude glycerol and algal biomass ($0.09 \text{ kJ/g-VS}_{\text{added}}$) [18]. Using a codigestion process, the biological conversion of crude glycerol and algal biomass at a concentration of 1 g-VS gained 1.27 kJ as energy. Under this condition, the overall substrate concentration was $30.22 \text{ g-VS}_{\text{added}}$. Hence, the energy production from a two-stage process should be $[1.27 \text{ kJ/g-VS}_{\text{added}} \times 30.22 \text{ g-VS}_{\text{added}}] = 38.38 \text{ kJ}$.

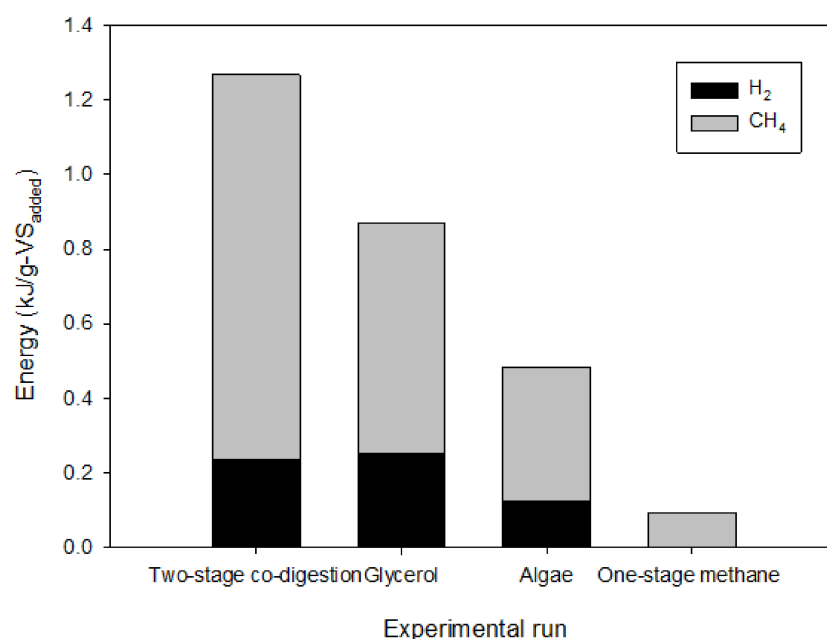


Figure 6. Energy production in two-stage hydrogen and methane production from the codigestion of crude glycerol and algal biomass and mono digestion of crude glycerol or algal biomass and one-stage methane production from the codigestion of crude glycerol and algal biomass [18].

Under the optimal conditions, the energy balance was calculated by subtracting output energy from input energy. At the optimum condition, the output energy was 38.38 kJ . Under these conditions, the substrate concentration and fermentation times were $30.22 \text{ g-VS}_{\text{added}}$ and 294 h , respectively. As a result, the input energy calculated based on Equation (7) was 5253 kJ . Hence, the net energy in two-stage hydrogen and methane production from a codigestion of crude glycerol with algal biomass was -5215 kJ . The high energy demand of the shaker (150 watt) was the main contributors to the high energy input, which resulted in negative net energy. An alternative low shaker consumption can be used to reduce the consumption of energy, making the process more energy efficient.

4. Conclusions

The results demonstrated that the codigestion of crude glycerol with algal biomass improved hydrogen and methane production. The variations in crude glycerol, algal biomass, and inoculum concentrations changed the microbial communities. The use of crude glycerol concentration, inoculum concentration, and algal biomass concentration at optimal levels enhanced microbial activity, resulting in maximal hydrogen and methane production. The use of a single substrate (crude glycerol only) provided a higher hydrogen

yield than the codigestion of crude glycerol with algal biomass. In contrast, the codigestion process provides a higher methane yield than the single digestion. Two-stage anaerobic digestion provided better energy production than one-stage anaerobic digestion.

Author Contributions: Conceptualization, A.R. and S.S.; methodology, N.S. and S.S.; investigation, A.R., P.P., N.S. and S.S.; formal analysis, N.S. and S.S.; writing—original draft preparation, S.S.; writing—review and editing, S.S. and A.R.; supervision, A.R. All authors have read and agreed to the published version of the manuscript.

Funding: This research project was supported by Mahidol University and Thammasat University Research Fund under the Research University Network (RUN) and TRF Senior Research Scholar (Grant No. RTA6280001). Partially funded by the National Research Council of Thailand.

Institutional Review Board Statement: Not applicable.

Informed Consent Statement: Not applicable.

Data Availability Statement: The datasets generated during and/or analyzed during the current study are available from the corresponding author on reasonable request.

Acknowledgments: The authors would like to thank the Research and Graduate Studies, Khon Kaen University for the support of this research.

Conflicts of Interest: The authors declare no conflict of interest.

References

1. Nazir, M.S.; Mahdi, A.J.; Bilal, M.; Sohail, H.M.; Ali, N.; Iqbal, H.M.N. Environmental impact and pollution-related challenges of renewable wind energy paradigm—A review. *Sci. Total Environ.* **2019**, *683*, 436–444. [[CrossRef](#)]
2. Gasanzade, F.; Pfeiffer, W.T.; Witte, F.; Tuschy, I.; Bauer, S. Subsurface renewable energy storage capacity for hydrogen, methane and compressed air— A performance assessment study from the north German basin. *Renew. Sustain. Energy Rev.* **2021**, *149*, 111422. [[CrossRef](#)]
3. Lanzilli, M.; Esercizio, N.; Vastano, M.; Xu, Z.; Nuzzo, G.; Gallo, C.; Manzo, E.; Fontana, A.; d’Ippolito, G. Effect of cultivation parameters on fermentation and hydrogen production in the phylum *Thermotogae*. *Int. J. Mol. Sci.* **2021**, *22*, 341. [[CrossRef](#)] [[PubMed](#)]
4. Mikheeva, E.R.; Khatraeva, I.V.; Kovalev, A.A.; Kovalev, D.A.; Nozhevnikova, A.N.; Panchenko, V.; Fiore, U.; Litt, Y.V. The start-up of continuous biohydrogen production from cheese whey: Comparison of inoculum pretreatment methods and reactors with moving and fixed polyurethane carriers. *Appl. Sci.* **2021**, *11*, 510. [[CrossRef](#)]
5. Maru, B.T.; Lopez, F.; Medina, F.; Constantí, M. Improvement of biohydrogen and usable chemical products from glycerol by co-culture of *Enterobacter* sp. H1 and *Citrobacter freundii* H3 using different supports as surface immobilization. *Fermentation* **2021**, *7*, 154. [[CrossRef](#)]
6. Romio, C.; Kofoed, M.V.W.; Møller, H.B. Digestate post treatment strategies for additional biogas recovery: A Review. *Sustainability* **2021**, *13*, 9295. [[CrossRef](#)]
7. Nualsri, C.; Reungsang, A.; Plangklang, P. Biochemical hydrogen and methane potential of sugarcane syrup using a two-stage anaerobic fermentation process. *Ind. Crop. Prod.* **2016**, *82*, 88–99. [[CrossRef](#)]
8. Hovorukha, V.; Havryliuk, O.; Gladka, G.; Tashyrev, O.; Kalinichenko, A.; Sporek, M.; Dołhańczuk-Śródka, A. Hydrogen dark fermentation for degradation of solid and liquid food waste. *Energies* **2021**, *14*, 1831. [[CrossRef](#)]
9. Bakonyi, P.; Dharmaraja, J.; Shobana, S.; Koók, L.; Rózsenszki, T.; Nemestóthy, N.; Banu, J.R.; Bélafi-Bakó, K.; Kumar, G. Leachate valorization in anaerobic biosystems: Towards the realization of waste to energy concept via biohydrogen, biogas and bioelectrochemical processes. *Int. J. Hydrog. Energy* **2019**, *44*, 17278–17296. [[CrossRef](#)]
10. Singh, R.; Tevatia, R.; White, D.; Demirel, Y.; Blum, P. Comparative kinetic modeling of growth and molecular hydrogen overproduction by engineered strains of *Thermotoga maritima*. *Int. J. Hydrog. Energy* **2019**, *44*, 7125–7136. [[CrossRef](#)]
11. Tan, X.B.; Zhao, X.C.; Yang, L.B. Strategies for enhanced biomass and lipid production by *Chlorella pyrenoidosa* culture in starch processing wastewater. *J. Clean. Prod.* **2019**, *236*, 117671. [[CrossRef](#)]
12. Sittijunda, S.; Reungsang, A. Valorization of crude glycerol into hydrogen, 1,3-propanediol, and ethanol in an up-flow anaerobic sludge blanket (UASB) reactor under thermophilic conditions. *Renew. Energy* **2020**, *161*, 361–372. [[CrossRef](#)]
13. Garlapati, V.K.; Shankar, U.; Budhiraja, A. Bioconversion technologies of crude glycerol to value added industrial products. *Biotechnol. Rep.* **2016**, *9*, 9–14. [[CrossRef](#)] [[PubMed](#)]
14. Dębowski, M.; Kisielewska, M.; Kazimierowicz, J.; Rudnicka, A.; Dudek, M.; Romanowska-Duda, Z.; Zieliński, M. The effects of microalgae biomass co-substrate on biogas production from the common agricultural biogas plants feedstock. *Energies* **2020**, *13*, 2186. [[CrossRef](#)]

15. Ganesh Saratale, R.; Kumar, G.; Banu, R.; Xia, A.; Periyasamy, S.; Dattatraya Saratale, G. A critical review on anaerobic digestion of microalgae and macroalgae and co-digestion of biomass for enhanced methane generation. *Bioresour. Technol.* **2018**, *262*, 319–332. [[CrossRef](#)] [[PubMed](#)]
16. Lu, D.; Zhang, X.J. Biogas production from anaerobic codigestion of microalgae and septic sludge. *J. Environ. Eng.* **2016**, *142*, 04016049. [[CrossRef](#)]
17. Thorin, E.; Olsson, J.; Schwede, S.; Nehrenheim, E. Co-digestion of sewage sludge and microalgae–Biogas production investigations. *Appl. Energy* **2018**, *227*, 64–72. [[CrossRef](#)]
18. Sittijunda, S.; Reungsang, A. Methane production from the co-digestion of algal biomass with crude glycerol by anaerobic mixed cultures. *Waste Biomass Valorization* **2020**, *11*, 1873–1881. [[CrossRef](#)]
19. AOAC International. *Official Methods of Analysis of AOAC International*, 19th ed.; AOAC International: Gaithersburg, MD, USA, 2012.
20. Phanduang, O.; Lunprom, S.; Salakkam, A.; Liao, Q.; Reungsang, A. Improvement in energy recovery from *Chlorella* sp. biomass by integrated dark-photo biohydrogen production and dark fermentation-anaerobic digestion processes. *Int. J. Hydrog. Energy* **2019**, *44*, 23899–23911. [[CrossRef](#)]
21. Lin, C.Y.; Lay, C.H. A nutrient formulation for fermentative hydrogen production using anaerobic sewage sludge microflora. *Int. J. Hydrog. Energy* **2005**, *30*, 285–292. [[CrossRef](#)]
22. Sittijunda, S.; Reungsang, A. Media optimization for biohydrogen production from waste glycerol by anaerobic thermophilic mixed cultures. *Int. J. Hydrog. Energy* **2012**, *37*, 15473–15482. [[CrossRef](#)]
23. Sittijunda, S.; Reungsang, A. Biohydrogen production from crude glycerol using anaerobic mixed cultures: Media compositions optimization. *Chiang Mai J. Sci.* **2018**, *45*, 653–667.
24. Sim, Y.B.; Jung, J.H.; Baik, J.H.; Park, J.H.; Kumar, G.; Rajesh Banu, J.; Kim, S.H. Dynamic membrane bioreactor for high rate continuous biohydrogen production from algal biomass. *Bioresour. Technol.* **2021**, *340*, 125562. [[CrossRef](#)]
25. Lay, J.J. Modeling and optimization of anaerobic digested sludge converting starch to hydrogen. *Biotechnol. Bioeng.* **2000**, *68*, 269–278. [[CrossRef](#)]
26. Owen, W.F.; Stuckey, D.C.; Healy, J.B.; Young, L.Y.; McCarty, P.L. Bioassay for monitoring biochemical methane potential and anaerobic toxicity. *Water Res.* **1979**, *13*, 485–492. [[CrossRef](#)]
27. Zwietering, M.H.; Jongenburger, I.; Rombouts, F.M.; van't Riet, K. Modeling of the bacterial growth curve. *Appl. Environ. Microbiol.* **1990**, *56*, 1875. [[CrossRef](#)] [[PubMed](#)]
28. Sreela-or, C.; Imai, T.; Plangklang, P.; Reungsang, A. Optimization of key factors affecting hydrogen production from food waste by anaerobic mixed cultures. *Int. J. Hydrog. Energy* **2011**, *36*, 14120–14133. [[CrossRef](#)]
29. Pott, R.W.M.; Howe, C.J.; Dennis, J.S. The purification of crude glycerol derived from biodiesel manufacture and its use as a substrate by *Rhodospseudomonas palustris* to produce hydrogen. *Bioresour. Technol.* **2014**, *152*, 464–470. [[CrossRef](#)] [[PubMed](#)]
30. Venkataramanan, K.P.; Boatman, J.J.; Kurniawan, Y.; Taconi, K.A.; Bothun, G.D.; Scholz, C. Impact of impurities in biodiesel derived crude glycerol on the fermentation by *Clostridium pasteurianum* ATCC 6013. *Appl. Microbiol. Biotechnol.* **2012**, *93*, 1325–1335. [[CrossRef](#)] [[PubMed](#)]
31. Ingram, L.O. Adaptation of membrane lipids to alcohols. *J. Bacteriol.* **1976**, *125*, 670–678. [[CrossRef](#)] [[PubMed](#)]
32. Cappai, G.; De Gioannis, G.; Muntoni, A.; Spiga, D.; Boni, M.R.; Poletti, A.; Pomi, R.; Rossi, A. Biohydrogen production from food waste: Influence of the inoculum to substrate ratio. *Sustainability* **2018**, *10*, 4506. [[CrossRef](#)]
33. Florio, C.; Pirozzi, D.; Ausiello, A.; Micoli, L.; Pasquale, V.; Toscano, G.; Turco, M.; Dumontet, S. Effect of inoculum/substrate ratio on dark fermentation for biohydrogen production from organic fraction of municipal solid waste. *Chem. Eng. Trans.* **2017**, *57*. [[CrossRef](#)]
34. Phanduang, O.; Lunprom, S.; Salakkam, A.; Reungsang, A. Anaerobic solid-state fermentation of bio-hydrogen from microalgal *Chlorella* sp. biomass. *Int. J. Hydrog. Energy* **2017**, *42*, 9650–9659. [[CrossRef](#)]
35. Lin, C.Y.; Lay, C.H. Effects of carbonate and phosphate concentrations on hydrogen production using anaerobic sewage sludge microflora. *Int. J. Hydrog. Energy* **2004**, *29*, 275–281. [[CrossRef](#)]
36. Huang, L.; Pan, X.R.; Wang, Y.Z.; Li, C.X.; Chen, C.B.; Zhao, Q.B.; Mu, Y.; Yu, H.Q.; Li, W.W. Modeling of acetate-type fermentation of sugar-containing wastewater under acidic pH conditions. *Bioresour. Technol.* **2018**, *248*, 148–155. [[CrossRef](#)]
37. Moreira, F.S.; Machado, R.G.; Romão, B.B.; Batista, F.R.X.; Ferreira, J.S.; Cardoso, V.L. Improvement of hydrogen production by biological route using repeated batch cycles. *Process. Biochem.* **2017**, *58*, 60–68. [[CrossRef](#)]
38. Choi, J.; Ahn, Y. Biohydrogen fermentation from sucrose and piggery waste with high levels of bicarbonate alkalinity. *Energies* **2015**, *8*, 1716–1729. [[CrossRef](#)]
39. Fountoulakis, M.S.; Manios, T. Enhanced methane and hydrogen production from municipal solid waste and agro-industrial by-products co-digested with crude glycerol. *Bioresour. Technol.* **2009**, *100*, 3043–3047. [[CrossRef](#)]
40. Kanchanasuta, S.; Sillaparassamee, O. Enhancement of hydrogen and methane production from co-digestion of palm oil decanter cake and crude glycerol using two stage thermophilic and mesophilic fermentation. *Int. J. Hydrog. Energy* **2017**, *42*, 3440–3446. [[CrossRef](#)]
41. Silva, F.M.S.; Oliveira, L.B.; Mahler, C.F.; Bassin, J.P. Hydrogen production through anaerobic co-digestion of food waste and crude glycerol at mesophilic conditions. *Int. J. Hydrog. Energy* **2017**, *42*, 22720–22729. [[CrossRef](#)]

42. Zahedi, S.; Solera, R.; García-Morales, J.L.; Sales, D. Effect of the addition of glycerol on hydrogen production from industrial municipal solid waste. *Fuel* **2016**, *180*, 343–347. [[CrossRef](#)]
43. Li, H.; Wang, Y. The effect of propionic acid accumulation on methane production in dry mesophilic anaerobic fermentation. *IOP Conf. Ser. Earth Environ. Sci.* **2021**, *675*, 12208. [[CrossRef](#)]
44. Jomnonkhaow, U.; Sittijunda, S.; Reungsang, A. Enhanced simultaneous saccharification and fermentation of Napier grass and Napier silage for two stage bio-hydrogen and methane production using organosolv and hydrothermal. *Mater. Chem. Phys.* **2021**, *267*, 124614. [[CrossRef](#)]
45. Krishnan, S.; Singh, L.; Sakinah, M.; Thakur, S.; Wahid, Z.A.; Alkasrawi, M. Process enhancement of hydrogen and methane production from palm oil mill effluent using two-stage thermophilic and mesophilic fermentation. *Int. J. Hydrog. Energy* **2016**, *41*, 12888–12898. [[CrossRef](#)]
46. Cibis, K.G.; Gneipel, A.; König, H. Isolation of acetic, propionic and butyric acid-forming bacteria from biogas plants. *J. Biotechnol.* **2016**, *220*, 51–63. [[CrossRef](#)]
47. Shrestha, P.M.; Malvankar, N.S.; Werner, J.J.; Franks, A.E.; Elena Rotaru, A.; Shrestha, M.; Liu, F.; Nevin, K.P.; Angenent, L.T.; Lovley, D.R. Correlation between microbial community and granule conductivity in anaerobic bioreactors for brewery wastewater treatment. *Bioresour. Technol.* **2014**, *174*, 306–310. [[CrossRef](#)] [[PubMed](#)]
48. Wu, J.; Jiang, B.; Kong, Z.; Yang, C.; Li, L.; Feng, B.; Luo, Z.; Xu, K.Q.; Kobayashi, T.; Li, Y.Y. Improved stability of up-flow anaerobic sludge blanket reactor treating starch wastewater by pre-acidification: Impact on microbial community and metabolic dynamics. *Bioresour. Technol.* **2021**, *326*, 124781. [[CrossRef](#)]
49. Yin, Z.; Bi, X.; Xu, C. Ammonia-oxidizing archaea (AOA) play with ammonia-oxidizing bacteria (AOB) in nitrogen removal from wastewater. *Archaea* **2018**, *2018*, 8429145. [[CrossRef](#)]
50. Quehenberger, J.; Shen, L.; Albers, S.V.; Siebers, B.; Spadiut, O. *Sulfolobus*—A potential key organism in future biotechnology. *Front. Microbiol.* **2017**, *8*, 2474. [[CrossRef](#)] [[PubMed](#)]
51. Himanshu, H.; Murphy, J.D.; Grant, J.; O’Kiely, P. Antagonistic effects on biogas and methane output when co-digesting cattle and pig slurries with grass silage in in-vitro batch anaerobic digestion. *Biomass Bioenergy* **2018**, *109*, 190–198. [[CrossRef](#)]